Coordination Chemistry Reviews 253 (2009) 2296–2305

Contents lists available at ScienceDirect

Coordination Chemistry Reviews

journal homepage: www.elsevier.com/locate/ccr

Review

2,6-Bis(hydroxymethyl)phenols for the synthesis of high-nuclearity clusters

Thorsten Glaser[a,*], Ioannis Liratzis[a], Ayuk M. Ako[b], Annie K. Powell[b,**]

[a] Lehrstuhl für Anorganische Chemie, Universität Bielefeld, Universitätsstr. 25, D-33615 Bielefeld, Germany
[b] Institut für Anorganische Chemie, Universität Karlsruhe (TH), Engesserstr. 15, D-76131 Karlsruhe, Germany

Contents

ARTICLE INFO

Article history:
Received 19 September 2008
Accepted 22 November 2008
Available online 3 December 2008

Keywords:
Polynuclear complexes
Molecular magnetism
Single-molecule magnets

ABSTRACT

Ligands based on 2,6-bis(hydroxymethyl)phenol H_3L^R possess three potential ligating groups either deprotonated or non-deprotonated: one phenol and two benzylalcohol groups. One important property of the benzylalcoholato function is its strong basicity mainly due to the lack of resonance stabilization of the corresponding anion. This leads to their pronounced tendency to bridge metal centers rather than to bind to one metal center in a terminal fashion. Therefore, ligands based on 2,6-bis(hydroxymethyl)phenol H_3L^R are well suited for the preparation of high-nuclearity complexes. The possible coordination modes of 2,6-bis(hydroxymethyl)phenol ligands H_3L^R have been summarized. Only the use of strong Lewis-acidic metal ions like Ti^{IV} enables a terminal coordination mode of the benzylalcoholato function as evidenced in the dinuclear complex $[(L^{t\text{-}Bu})_3Ti_2]^-$, **$[Ti_2]^-$**. This complex is in protic solvents in an equilibrium with the tetranuclear complex $[(L^{t\text{-}Bu})_2(HL^{t\text{-}Bu})_4Ti_4O_2]^{2-}$, **$[Ti_4]^{2-}$**. In the latter, the deprotonated benzylalcohol function of the ligand $(HL^{t\text{-}Bu})^{2-}$ bridges two Ti^{IV} ions demonstrating a small energy difference for a terminal and a bridging coordination mode of the benzylalcoholate to Ti^{IV}. For the less Lewis-acidic Fe^{III} ion, only a bridging coordination of benzylalcoholate has been found in a tetranuclear complex, $[(HL^{t\text{-}Bu})_6Fe^{III}{}_4(acac)_2]^{2-}$, **$[Fe^{III}{}_4]^{2-}$**, a decanuclear complex, $[(HL^{t\text{-}Bu})_{12}Fe_{10}Na_4(\mu_3\text{-}O)_4(\mu_3\text{-}OH)_2(dme)_2(EtOH)_2]$, **$[Fe^{III}{}_{10}]$**, and a dinuclear complex, $[(HL^{t\text{-}Bu})_4Fe^{III}(\mu_2\text{-}CO_3)]^{4-}$, **$[Fe^{III}{}_2]^{4-}$**. The exchange interactions in these complexes are all antiferromagnetic leading to diamagnetic $S_t = 0$ spin ground states. On the other hand, the reaction of H_3L^{Me} with Mn^{II} in the presence of N_3^- results in the nonadecanuclear mixed valence complex $[(HL^{Me})_{12}Mn^{III}{}_{12}Mn^{II}{}_7(\mu_4\text{-}O)_8(\mu_3,\eta^1\text{-}N_3)_8(MeCN)_6]^{2+}$, **$[Mn^{III}{}_{12}Mn^{II}{}_7]^{2+}$**, which exhibits ferromagnetic interactions with the maximum $S_t = 83/2$ spin ground state—the highest spin yet established in a molecule. These results demonstrate the potential of 2,6-bis(hydroxymethyl)phenol ligands for the synthesis of high-nuclearity clusters with interesting magnetic properties.

1. Introduction

The considerable interest in the synthesis of magnetic materials based on molecular entities with potential application in fields such as molecular electronics [1–5] began with the observation that $[Cp^*_2Fe]^+[TCNE]^-$ exhibits a spontaneous long-range ferromagnetic ordering with a Curie temperature T_C of 4.8 K [6,7]. In this respect, it is important to differentiate between the field of molecular magnetism in general and molecule-based magnets in

* Corresponding author. Tel.: +49 521 106 6105; fax: +49 521 106 6003.
** Corresponding author. Tel.: +49 721 608 2135; fax: +49 721 608 8142.
E-mail addresses: thorsten.glaser@uni-bielefeld.de (T. Glaser), powell@aoc.uni-karlsruhe.de (A.K. Powell).

0010-8545/$ – see front matter © 2008 Elsevier B.V. All rights reserved.
doi:10.1016/j.ccr.2008.11.014

specific. The quite mature field of molecular magnetism deals with the properties of mononuclear or polynuclear transition metal complexes [8]. In the latter, a strong focus is on the exchange interaction between the paramagnetic centers in the polynuclear complexes. Despite these intramolecular interactions there are only very weak intermolecular interactions between the molecules and therefore the bulk samples are only paramagnetic; they exhibit no magnetization without an applied magnetic field. Compounds that are synthesized from molecular building blocks under the typical mild reaction conditions of molecular chemistry but which exhibit a hysteresis in the magnetization and which remain a magnetization at zero external fields are magnets in analogy to solid-state magnets and are termed molecule-based magnets.

The structure of $[Cp^*_2Fe]^+[TCNE]^-$ consists of chains of alternating $[Cp^*_2Fe]^+$ and $[TCNE]^-$ units both having a $S = 1/2$ ground state. The intrachain interaction is ferromagnetic with $J = +13\ cm^{-1}$ (all coupling constants J in this article are related to the Heisenberg–Dirac-van Vleck–Hamiltonian in the form of $H = -2J\ \mathbf{S}_1\mathbf{S}_2$). Below 4.8 K, weak but ferromagnetic dipolar interactions between the chains lead to the observed spontaneous magnetization. This 3D long-range magnetic order in a system constructed from molecular building blocks initiated world-wide research activities to prepare quasi-1D, 2D, and 3D molecule-based magnets. Important examples displaying Curie temperatures, T_C, above room temperature are $V(TCNE)_2 \cdot y(CH_2Cl_2)$ [9] and some of the members of the family of Prussian Blue analogues such as $K V^{II}[Cr^{III}(CN)_6]$ [10] or $V^{II}_{0.42}V^{III}_{0.58}[Cr^{III}(CN)_6]_{0.86} \cdot 2.8H_2O$ [11,12].

Another milestone in the field of molecule-based magnets was the observation that $[Mn_{12}O_{12}(O_2CCH_3)_{16}(OH_2)_4]$, **$Mn_{12}$** [13] exhibits a hysteresis in the magnetization of purely molecular origin and represents the first member of a new class of molecular materials called single-molecule magnets or SMMs [14–20]. In contrast to the molecule-based magnets mentioned above, which exhibit a long-range ferromagnetic order, SMMs possess an energy barrier for spin reversal which causes a slow relaxation of the magnetization at low temperatures. The energy barrier originates from a high spin ground state and a magnetic anisotropy of the easy-axis type with a negative zero-field splitting parameter D. **Mn_{12}** is a high spin molecule with an $S_t = 10$ spin ground state and a zero-field splitting D of $-0.5\ cm^{-1}$ resulting in a barrier to spin reversal of $D \cdot S_t^2$ of $\sim 50\ cm^{-1}$. This magnetic anisotropy barrier results in a magnetic bistability at low temperatures which has attracted a great deal of scientific attention [21] and several papers on the potential application of SMMs have appeared in the literature [22–26].

Since this discovery a great deal of research effort has been devoted to the synthesis of high-nuclearity transition metal clusters in the hope of achieving high spin ground states [27–35]. One successful strategy is the application of the acid–base-dependent oligo- and polymerization of transition metal ions to oxo-, hydroxy-, and alkoxy-bridged species [36,37]. In order to inhibit precipitation of the parent 2D and 3D oxides, hydroxides, or alkoxides the oligomerization is performed in the presence of capping ligands which prevent the formation of these extended lattices and give rise to large molecular clusters which, in contrast to the molecule-based ferromagnetic materials described above, can be described as 0D systems.

We review here the concerted synthetic efforts to evaluate the potential of 2,6-bis(hydroxymethyl)phenols as a ligand system for the preparation of discrete polynuclear metal complexes in the frame of the research program on Molecular Magnetism funded by the Deutsche Forschungsgemeinschaft. We will only consider ligands of the general formula H_3L^R with a substituent R at the 4-position and hydrogen atoms at 3- and 5-positions. Examples of other research groups will also be briefly described.

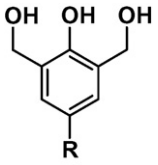

H_3L^R

2. The potential of *ortho*-bis(hydroxymethyl)phenols

The ligand H_3L^R is formally closely related to the ligand systems based on 2,6-bis(aminomethyl)phenol (**A**) and 2,6-bis(iminomethyl)phenol (**B**) backbones, which have been extensively employed for the synthesis of transition metal complexes. Ligands based on **A** or **B** are mainly dinucleating ligands, a concept introduced in 1970 by Robson and called compartmental or Robson-type ligands [38,39]. Since then, there has been a steady increase in the numbers and types of such ligands synthesized both in acyclic or macrocyclic versions. The synthesis of homo- and hetero-dinuclear transition metal complexes enabled detailed investigations of their magnetochemical and electrochemical properties. These studies provided important insights into the molecular and electronic structure of dinuclear metallo-proteins, and into the cooperativity of such sites in catalysis [40].

The related ligand 2,6-bis(hydroxymethyl)pyridine **C** has been used for the synthesis of polynuclear manganese complexes, which exhibit SMM behaviour [41,42].

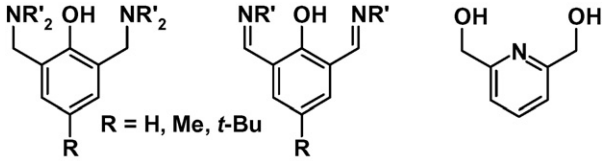

A **B** **C**

Despite structural similarities, the ligand system based on H_3L^R has only recently been used for the synthesis of transition metal complexes [43–48]. This may be related to a fundamental difference of the two benzylalcohol groups in H_3L^R in comparison to the amino- and imino-functions in **A** and **B**, respectively, which is that the benzylalcohol groups are able to coordinate to a metal ion both in its neutral BzOH and deprotonated BzO^- form due to the presence of several lone pairs, whereas the amino- and imino-functions of **A** and **B** possess only one lone pair. The several lone pairs enable the BzOH and BzO^- functions to coordinate to more than one metal, i.e., to function as a bridging ligand. This is not possible for amines and imines. Comparing BzO^- to the corresponding PhO^-, an important property of the deprotonated form BzO^- is its strong basicity, which is mainly due to the lack of resonance stabilization of the anion, compared with that of PhO^-. This leads to the more pronounced tendency of BzO^- to bridge [41,42,49,50] rather than to bind to one metal center in a terminal fashion, which is the usual coordination mode of amine and imine nitrogen donors. Therefore, the coordination chemistry of ligand types **A** and **B** is dominated by dinuclear metal complexes whereas ligands of type H_3L^R are well suited for the preparation of a variety of high-nuclearity complexes with differing coordination modes (Scheme 1).

The pK_s values of phenols are lower than those of benzyl alcohols. Thus, the mono-deprotonated form $(H_2L^R)^-$ should coordinate a metal ion via its phenolate oxygen atom (mode **I**) with a possible stabilization of a neutral benzylalcohol (mode **II**). There are many possible coordination modes for the doubly deprotonated form $(HL^R)^{2-}$ (modes **III**–**VIII**) ranging from mononuclear to trinuclear

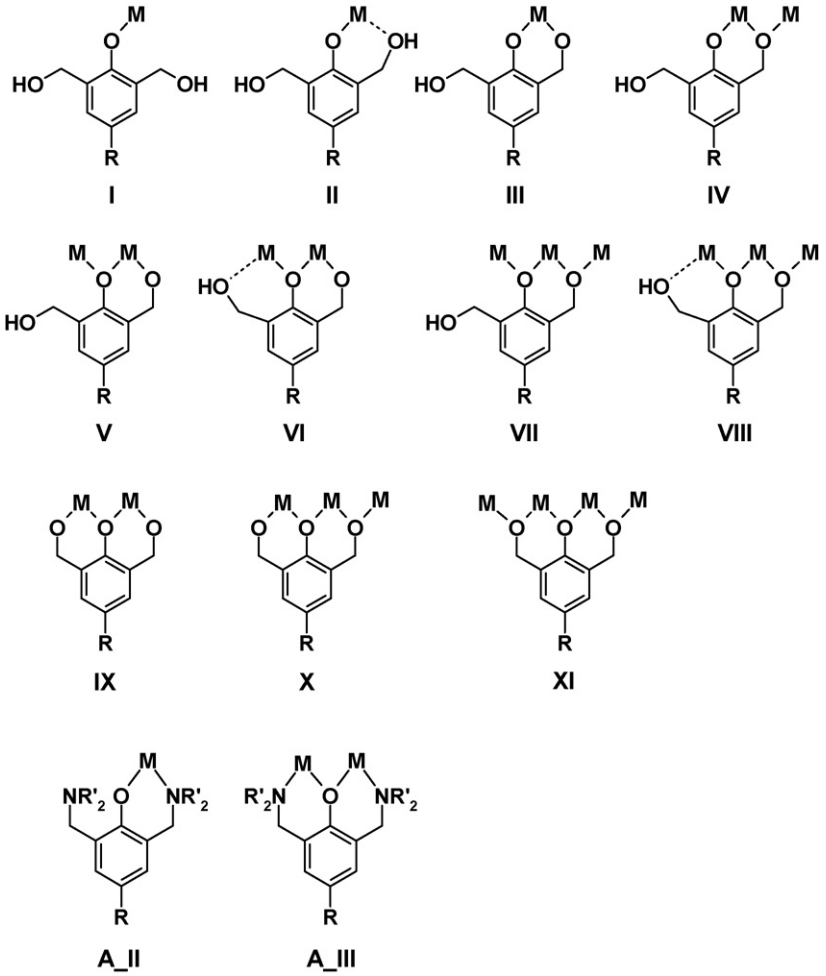

Scheme 1.

coordination fragments. For the dinuclear complex fragments, the electronic characteristics of the $(HL^R)^{2-}$ should prefer coordination mode **IV** in comparison to mode **V**. The negative charge of the deprotonated phenolate oxygen atom can be stabilized by delocalization through the benzene ring, while the negative charge of the deprotonated benzyl alcoholate oxygen atom is mainly localized on the oxygen atom. This should result in a higher tendency to bridge metal ions for the benzyl alcoholate in comparison to the phenolate group. However, stabilization as seen in mode **VI** or by characteristics of the ligands on the other positions may overcome these intrinsic characteristics of $(HL^R)^{2-}$. The tris-deprotonated form $(L^R)^{3-}$ may coordinate two, three, or four metal ions (modes **IX**, **X**, and **XI**, respectively). In addition, as a result of the rigidity of the backbone, it is not possible for $(L^R)^{3-}$ to coordinate with its three deprotonated oxygen atoms to one metal ion. The coordination mode **XI** could lead to one-dimensional chains with strongly interacting metal ions which could lead to interesting electronic and magnetic properties [51]. Dinuclear complexes with $(L^R)^{3-}$ in coordination mode **IX** could also function as molecular building blocks via the 'complexes as ligands' concept, for such one-dimensional chains. On the other hand, only two coordination modes seem feasible for ligands **A** and **B** (Scheme 1, only drawn for **A**).

In summary, the ligand H_3L^R has a plethora of possible coordination modes in comparison to the mainly dinucleating ligands **A** and **B**. The different protonation forms depend strongly on metal ions, solvents, coligands and the presence and strengths of acid and bases, so that it is difficult to predict *a priori* the structures which might result. The bridging ability of the various protonated forms in combination with its inability to chelate to one metal ion should allow for the isolation of a multitude of possible polynuclear complexes. For these reasons we embarked on an exploration of the coordination chemistry of H_3L^R with Ti^{IV}, Fe^{III}, and Mn^{III}.

3. Titanium complexes

Reaction of $H_3L^{t\text{-}Bu}$ with $[TiO(acac)_2]$ in the molar ratio 3:2 in the presence of Et_3N in MeOH under reflux yielded after addition of excess $(Et_4N)Cl$ yellow crystals of **1** [46]. The reaction of $H_3L^{t\text{-}Bu}$ and $[TiO(acac)_2]$ using similar conditions as for the synthesis of **1**, but stirring the reaction solution at room temperature, yielded yellow needles of **2** [46]. IR spectroscopy was found to be a useful tool to differentiate between the two complexes. The IR spectrum of **1** exits two strong absorptions for the stretching frequencies of the phenolic C–O bond at 1252 and 1212 cm^{-1} and one broad absorption of the benzylic C–O bond at 1041 cm^{-1}. Three strong well-resolved absorptions at 613, 590, and 564 cm^{-1} (ν(Ti–O)) can be taken as evidence for the coordination of the ligand to titanium. On the other hand, the IR spectrum of **2** exhibits a broad flat absorption at 2600–3200 cm^{-1} indicating that the ligand is not in its completely deprotonated form $(L^{t\text{-}Bu})^{3-}$. The phenolic C–O stretching region exhibits four absorptions with a different intensity pattern as compared to the two absorptions observed in the spectrum of **1**, while the absorption corresponding to the stretching frequency of the benzylic C–O bond at 1040 cm^{-1} becomes smaller and broadens in the spectrum of **2**. The three sharp well-resolved absorptions corresponding to the ν(Ti–O) stretches in the spectrum of **1** are

replaced by several poorly resolved transitions in this region of the spectrum of **2**. Thus, the IR spectrum of **2** indicates a less symmetric coordination mode of the ligand compared with **1** and/or the occurrence of more than one kind of coordination mode of the ligands.

The diamagnetic Ti^{IV} ion also allows study by NMR spectroscopy. The ^{1}H and ^{13}C NMR spectra of **1** correspond to a symmetrical coordination of only one kind of trianionic ligand $(L^{t\text{-}Bu})^{3-}$. The ^{1}H NMR spectrum of **2** is more complex. The observation of three *tert*-butyl resonances and six different signals for the aromatic protons demonstrate the presence of three distinguishable sets of ligand molecules in **2**. Additionally, two resonances corresponding to the hydroxy protons suggest that only seven of the nine possible hydroxy groups of the three ligand molecules are deprotonated in **2**. In the region of the benzylic resonances there is a multitude of sharp signals indicating that the two protons of each benzylic group are inequivalent and that no fluctuational interconversion between them occurs.

Structural analysis by single-crystal diffraction confirmed the predictions from the spectroscopic data. Compound **1** was established to be $(NEt_4)[(L^{t\text{-}Bu})_3Ti_2]$ containing the symmetric bioctahedral $[(L^{t\text{-}Bu})_3Ti_2]^-$ anion, $\mathbf{[Ti_2]^-}$. Fig. 1 shows two views of the molecular structure of the anion $\mathbf{[Ti_2]^-}$. Each ligand acts as a tridentate donor with two terminal phenylmethoxide donors (BzO^-) and one μ_2-bridging phenolate donor (PhO^-) corresponding to coordination mode **IX**. The two titanium ions are bridged in a face-sharing fashion by the three phenolato donors giving rise to an overall bioctahedral core. The $Ti_1\cdots Ti_2$ distance is 3.03 Å. The Ti–μ_2-OPh bond distances are in the range 2.10–2.13 Å while the Ti–OBz bond distances are 0.3 Å shorter (1.81–1.84 Å). The short Ti–OBz bond distances indicate a highly covalent bond between the strong Lewis acidic Ti^{IV} ions and the strong Lewis basic BzO^-, which exhibit no resonance stabilization of the negative charge as compared to PhO^-.

Single-crystal X-ray diffraction established that **2** consists of tetranuclear dianions $[(L^{t\text{-}Bu})_2(HL^{t\text{-}Bu})_4Ti_4O_2]^{2-}$, $\mathbf{[Ti_4]^{2-}}$, and Et_4N^+ cations. The molecular structure of $\mathbf{[Ti_4]^{2-}}$ may be regarded as a Ti_4O_{16} core decorated by an organic shell (Fig. 2, left). The oxygen atoms lie above and below a plane constructed from the four titanium ions (Fig. 2, right). In the crystal structure of **2**, two hydrophobic pockets are formed by three *t*-butylbenzene groups that are occupied by the two Et_4N^+ cations.

Two oxygen atoms of the Ti_4O_{16} core are provided by oxide anions, six derive from phenolates and eight from benzyl alcoholates. Two of the ligands are in the triple-deprotonated form $(L^{t\text{-}Bu})^{3-}$ and coordinate in mode **IX**. The other four ligands are in the double-deprotonated form $(HL^{t\text{-}Bu})^{2-}$. Two of these coordinate in mode **III** and the other two in mode **IV**. The four protonated benzylalcohol groups stabilize the whole complex by forming intramolecular hydrogen bonds with the four terminally coordinated benzyl alcoholate groups.

The mean bond distances for the different kinds of Ti–O bonds are: Ti–OBz 1.86 Å, Ti–OPh 1.90 Å, Ti–μ_3-O 1.97 Å, Ti–μ_2-OBz 2.03 Å, and Ti–μ_2-OPh 2.08 Å. The terminal phenylmethoxide donors form the shortest Ti–O bonds while the bridging phenolato donors form the longest Ti–O bonds. It is interesting to compare these values with the corresponding values for Ti–OBz (1.83 Å) and Ti–μ_2-OPh (2.11 Å) found in **1**: the Ti–OBz bonds are a bit shorter in **1** compared with **2** and the Ti–μ_2-OPh are a bit longer in **1**. There are two other trends observed in the bond distances in **2**. Firstly, the Ti–O bond distance of one type of oxygen donor decreases on going from monodentate to bridging, consistent with a bridging ligand having to donate more total charge leading to less charge donation per bond [52,53], and secondly the Ti–O bond distance of a phenylmethoxide donor is shorter than a phenolato donor of the same coordination mode (OBz vs. OPh and μ_2-OBz vs. μ_2-OPh). This is consistent with the stronger donor ability of a phenylmethoxide ligand compared with a phenolato ligand as a result of the difference in resonance stabilization of the anion [54].

Although, IR, NMR, and X-ray diffraction established different structures for **2** and **1**, the electrospray mass spectrum of **2** in MeOH exhibits only the prominent ion corresponding to $[(L^{t\text{-}Bu})_3Ti_2]^-$. This indicates the transformation of $\mathbf{[Ti_4]^{2-}}$ into $\mathbf{[Ti_2]^-}$ under the conditions of the electrospray ionization (high-temperature). Further studies of **1** and **2** in solution demonstrate the presence of an equilibrium between $\mathbf{[Ti_4]^{2-}}$ and $\mathbf{[Ti_2]^-}$ (Eq. (1)).

$$\underset{\mathbf{[Ti_4]^{2-}}}{[(L^{t\text{-}Bu})_2(HL^{t\text{-}Bu})_4Ti_4O_2]^{2-}} \leftrightarrows 2\,\underset{\mathbf{[Ti_2]^-}}{[(L^{t\text{-}Bu})_3Ti_2]^-} + 2\,H_2O \quad (1)$$

Heating $\mathbf{Ti_4^{2-}}$ in protic solvents leads to the formation of $\mathbf{[Ti_2]^-}$, an essential feature for the controlled synthesis of **1** and **2**. Thus, heating a methanolic solution of $\mathbf{Ti_4^{2-}}$ in the process of the ESI measurement results in the formation of $\mathbf{[Ti_2]^-}$. $\mathbf{[Ti_4]^{2-}}$ is stable in non-protic solvents even upon heating. In addition, it was found that $\mathbf{[Ti_2]^-}$ can be converted back to $\mathbf{[Ti_4]^{2-}}$. If $\mathbf{[Ti_2]^-}$ is maintained in a CH_3CN/MeOH mixture (10:1) yellow crystals of **2** result. These observations suggest that the cleavage of the titanium-oxo bond of the former titanyl unit requires an activation energy and a protic solvent is needed to enable the formation of water according to Eq. (1). The dinuclear $[(L^{t\text{-}Bu})_3Ti_2]^-$ complex seems to be more stable in protic solvents, whereas the tetranuclear $[L^{t\text{-}Bu}{}_2(HL^{t\text{-}Bu})_4Ti_4O_2]^{2-}$ complex seems to be more stable in aprotic solvents.

A tetranuclear titanium complex closely related to $\mathbf{[Ti_4]^{2-}}$ was reported by Henry and coworkers in two different solvates using the methyl-derivative H_3L^{Me} [43]. Interestingly, the constitution and molecular structure of that complex resembles that of $\mathbf{[Ti_4]^{2-}}$ despite being a neutral complex. Thus, two additional protons have to be present in comparison to $\mathbf{[Ti_4]^{2-}}$. Bond valence sum argumentations indicate that two of the ligands, that chelate in coordination mode **III** in $\mathbf{[Ti_4]^{2-}}$, are actually monoanionic ligands $(H_2L^{Me})^-$ that coordinate in mode **II** in the complex of Henry and coworkers. This complex possesses the ligand in the three different protonation forms $(L^{Me})^{3-}$, $(HL^{Me})^{2-}$, and $(H_2L^{Me})^-$ and the formulation is as $[(L^{Me})_2(HL^{Me})_2(H_2L^{Me})_2Ti_4O_2]$.

4. Iron complexes

The reaction of the ligand $H_3L^{t\text{-}Bu}$ with Fe^{III} under a range of conditions afforded complexes of various nuclearity. A tetranuclear complex of butterfly topology was obtained by reacting $H_3L^{t\text{-}Bu}$ with $Fe(acac)_3$ and NEt_3 in acetonitrile using anhydrous and anaerobic conditions: $[HNEt_3]_2[(HL^{t\text{-}Bu})_6Fe^{III}{}_4(acac)_2]$ [44].

The tetranuclear complex $[(HL^{t\text{-}Bu})_6Fe^{III}{}_4(acac)_2]^{2-}$, $\mathbf{[Fe^{III}{}_4]^{2-}}$, possesses an $\{Fe_4O_{16}\}$ core decorated by an organic shell (Fig. 3). All ligands are in the doubly deprotonated form $(HL^{t\text{-}Bu})^{2-}$ and coordinate to the Fe^{III} ions in mode **IV**. The neutral protonated benzylalcohol groups form intra- and intermolecular hydrogen bonds to coordinated oxygen atoms. The intermolecular hydrogen bonds lead to the formation of a staircase one-dimensional chain in the solid state.

The effective magnetic moment, μ_{eff}, decreases with decreasing temperature indicative of intramolecular antiferromagnetic interactions with an $S_t = 0$ spin ground state (Fig. 4). The spin topology of $\mathbf{[Fe^{III}{}_4]^{2-}}$ resembles that of previously described 'butterfly' complexes [55–57]. The magnetic data were analyzed using the spin-Hamiltonian (Eq. (2)) taking into account all relevant exchange coupling pathways (i.e., in the butterfly-nomenclature the so-called wing-body coupling J_{wb} and the body–body

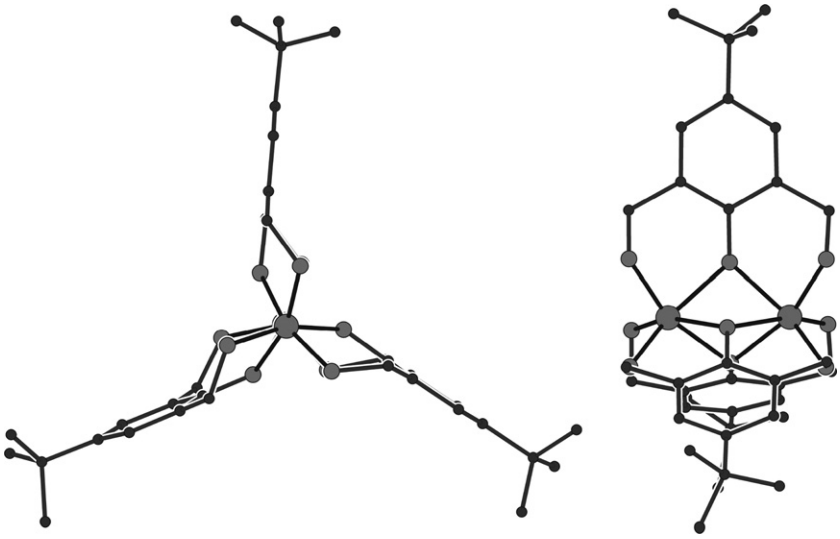

Fig. 1. Molecular structure of the monoanion $[(L^{t\text{-}Bu})_3Ti_2]^-$, **[Ti$_2$]$^-$**, in **1** along the Ti–Ti vector (left) and perpendicular to the Ti–Ti vector (right). The ligand only occurs in coordination mode **IX**.

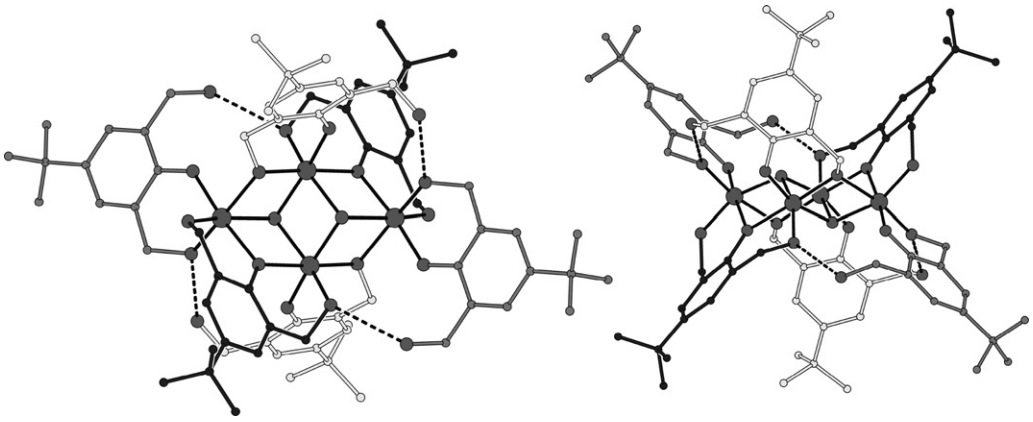

Fig. 2. Molecular structure of the dianion $[(L^{t\text{-}Bu})_2(HL^{t\text{-}Bu})_4Ti_4O_2]^{2-}$, **[Ti$_4$]$^{2-}$**, in **2** perpendicular to the Ti_4O_{16} core 'layer' (left) and along this 'layer' (right). The six ligands occur in three different coordination modes: mode **III** (grey), mode **IV** (light grey), and mode **IX** (dark grey). Intramolecular hydrogen-bonds are indicated by dashed lines.

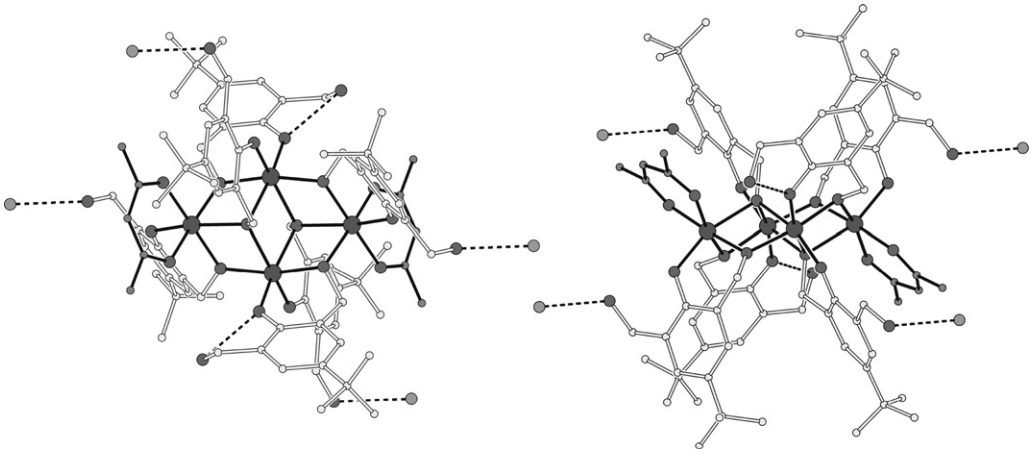

Fig. 3. Molecular structure of the dianion $[(HL^{t\text{-}Bu})_6Fe^{III}{}_4(acac)_2]^{2-}$ in **[Fe$^{III}_4$]$^{2-}$** perpendicular to the Fe_4O_{16} core 'layer' (left) and along this 'layer' (right). All six ligands are double-deprotonated and coordinate in the same mode **IV**. Hydrogen-bonds are indicated by dashed lines.

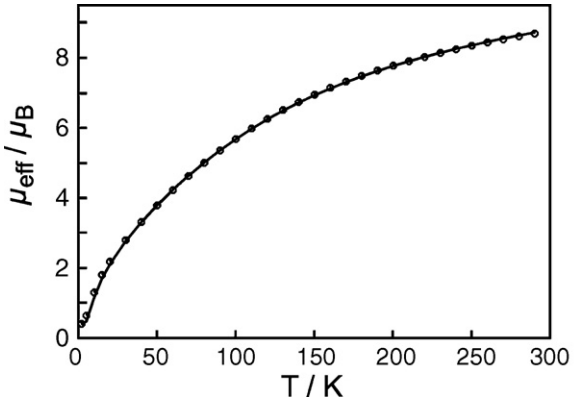

Fig. 4. Temperature dependence of the effective magnetic moment, μ_{eff}, of $[HNEt_3]_2[(HL^{t\text{-}Bu})_6Fe^{III}{}_4(acac)_2]$ at 1 T (the solid line is a fit to the experimental data using spin-Hamiltonian (2) with $J_{wb} = -10.0\,cm^{-1}$ and $J_{bb} = -6.2\,cm^{-1}$).

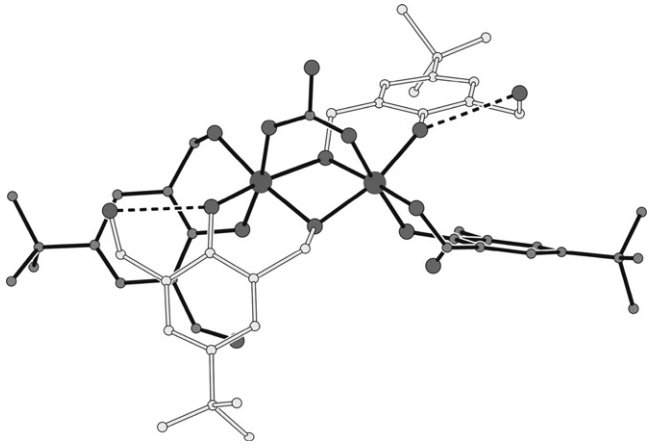

Fig. 6. Molecular structure of $[(HL^{t\text{-}Bu})_4Fe^{III}(\mu_2\text{-}CO_3)]^{4-}$, $\mathbf{[Fe^{III}{}_2]^{4-}}$. All four ligands are double-deprotonated and coordinated in two different modes: **III** (dark grey) and mode **IV** (light grey). Hydrogen bonds are indicated by dashed lines.

coupling J_{bb}).

$$H = -2J_{wb}(\boldsymbol{S}_2\boldsymbol{S}_1 + \boldsymbol{S}_2\boldsymbol{S}_{1'} + \boldsymbol{S}_{2'}\boldsymbol{S}_1 + \boldsymbol{S}_{2'}\boldsymbol{S}_{1'}) - 2J_{bb}\boldsymbol{S}_1\boldsymbol{S}_{1'} + \sum_{i=1}^{4}\left[D_i\left(\hat{S}_{zi}^2 - \frac{1}{3}S_i(S_i+1)\right) + \mu_B\boldsymbol{S}_i\boldsymbol{g}\boldsymbol{B}\right] \quad (2)$$

The analysis provided two main exchange pathways via the dialcoholato bridged Fe^{III} ions. The coupling of the two central ('body') Fe^{III} ions through the $(\mu_3\text{-}OBz)_2$ unit was found to be smaller with $J_{bb} = -6.2\,cm^{-1}$ in comparison to the coupling between a central and a terminal ('wing-tip') Fe^{III} ion with $J_{wb} = -10.0\,cm^{-1}$, which is mediated by one μ_3-OBz and one μ_2-OBz bridge. This is in agreement with shorter bond distances for Fe–μ_2-OBz bonds of 1.98 Å in comparison with the Fe–μ_3-OBz bonds at 2.13–2.15 Å.

Reaction of $H_3L^{t\text{-}Bu}$ with $Fe^{III}(ClO_4)_3{\cdot}10H_2O$ in ethanol with NaOH in the presence of dme yielded red crystals which were analyzed by single-crystal X-ray diffraction establishing the molecular structure $[(HL^{t\text{-}Bu})_{12}Fe_{10}Na_4(\mu_3\text{-}O)_4(\mu_3\text{-}OH)_2(dme)_2(EtOH)_2]$, $\mathbf{[Fe^{III}{}_{10}]}$ (Fig. 5) [45].

The inner $\{Fe_{10}O_{30}\}$ can be regarded as a portion of the γ-Fe·O·OH or lepidocrocite structure. The 12 ligands are in the doubly deprotonated form $(HL^{t\text{-}Bu})^{2-}$ but coordinate in different modes. Two ligands coordinate in mode **IV**. The uncoordinated benzylalcohol groups form intermolecular hydrogen bonds, resulting in an overall 2D network in the crystal structure (not shown). The additional coordination of two Na^+ ions to the phenolate oxygen atoms means that these ligands coordinate via mode **VII**. The remaining eight ligands have the same metal ion coordination but now the additional benzylalcohol group is no longer dangling but coordinated to a Na^+ resulting in coordination mode **VIII**.

Solution state studies establish that the molecular structure of $\mathbf{[Fe^{III}{}_{10}]}$ is not maintained in solution. The temperature dependence of μ_{eff} indicates overall antiferromagnetic interactions with an $S_t = 0$ spin ground state. However, the low temperature part of the data appeared to be sample-dependent, which might the result of differing amounts of paramagnetic impurities. Therefore, we refrain from a more detailed description on the magnetic properties of $\mathbf{[Fe^{III}{}_{10}]}$.

By carrying out the reaction of $H_3L^{t\text{-}Bu}$ with $Fe^{III}(ClO_4)_3{\cdot}10H_2O$ and NaOH in methanol, light red crystals were obtained and the structure was established by X-ray diffraction as $Na_4[(HL^{t\text{-}Bu})_4Fe^{III}(\mu_2\text{-}CO_3)]{\cdot}11MeOH{\cdot}2H_2O$ [45]. The molecular structure of the tetraanion $\mathbf{[Fe^{III}{}_2]^{4-}}$ is shown in Fig. 6.

The four ligands are in the doubly deprotonated form $(HL^{t\text{-}Bu})^{2-}$ and coordinate in two different modes. Two ligands coordinate in mode **IV** and two ligands in mode **III**. The uncoordinated as well as the coordinated oxygen atoms are involved in hydrogen bonding to disordered solvent molecules, which in combination with the

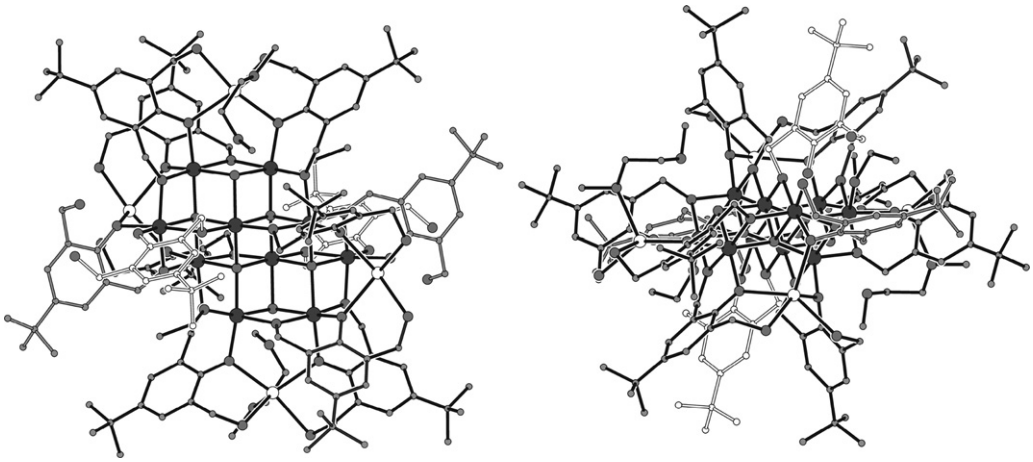

Fig. 5. Molecular structure of $[(HL^{t\text{-}Bu})_{12}Fe^{III}{}_{10}Na_4(\mu_3\text{-}O)_4(\mu_3\text{-}OH)_2(dme)_2(EtOH)_2]$, $\mathbf{[Fe^{III}{}_{10}]}$, perpendicular to the $Fe_{10}O_{30}$ core 'layer' (left) and along this 'layer' (right). The Na^+ ions are represented by white spheres. All 12 ligands are double-deprotonated. The 12 ligands occur in three different coordination modes: mode **IV** (light grey), mode **VII** (grey), and mode **VIII** (dark grey).

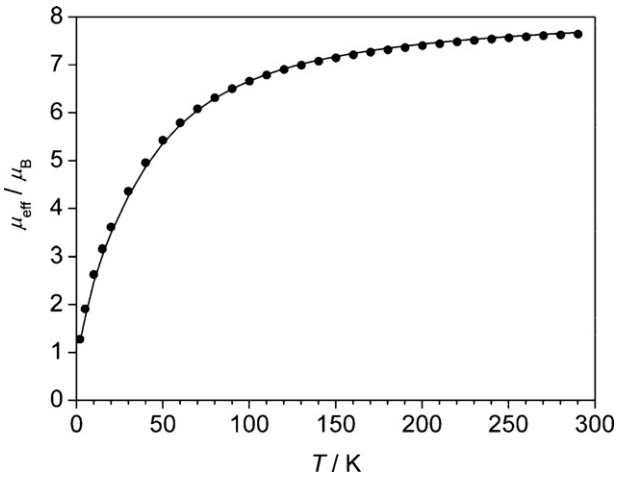

Fig. 7. Temperature dependence of the effective magnetic moment, μ_{eff}, of $Na_4[(HL^{t\text{-}Bu})_4Fe^{III}(\mu_2\text{-}CO_3)]\cdot 11MeOH\cdot 2H_2O$ at 1 T. The solid line is a fit to the experimental data with $J = -4.4\,cm^{-1}$.

four Na^+ counter ions results in a staircase chain within the crystal structure.

An interesting feature in the structure of **$[Fe^{III}_2]^{4-}$** is the incorporation of atmospheric CO_2 in form of CO_3^{2-} due to the strong basic conditions. This lead to the unprecedented $[Fe^{III}(\mu_2\text{-}OR)_2(\mu_2\text{-}CO_3)Fe^{III}]^{2+}$ core. The effective magnetic moment, μ_{eff}, decreases with decreasing temperature indicative of intramolecular antiferromagnetic interactions with an $S_t = 0$ spin ground state (Fig. 7). Fitting of the data result in a moderate antiferromagnetic coupling of $J = -4.4\,cm^{-1}$.

5. Manganese complexes

Reaction of H_3L^{Me} with $Mn^{II}Cl_2\cdot 4H_2O$ in the presence of NaN_3 and NaOAc in MeCN/MeOH afforded the unprecedented nonadecanuclear complex $[(HL^{Me})_{12}Mn^{III}{}_{12}Mn^{II}{}_7(\mu_4\text{-}O)_8(\mu_3,\eta^1\text{-}N_3)_8(MeCN)_6]Cl_2\cdot 10MeOH\cdot MeCN$. The molecular structure of the dication $[(HL^{Me})_{12}Mn^{III}{}_{12}Mn^{II}{}_7(\mu_4\text{-}O)_8(\mu_3,\eta^1\text{-}N_3)_8(MeCN)_6]^{2+}$, **$[Mn^{III}_{12}Mn^{II}_7]^{2+}$** (Fig. 8) is comprised of two $[Mn_{10}]$ supertetrahedra sharing a Mn^{II} vertex. Each of these is built up from a central octahedron of six Mn^{III} centers, of which four tetrahedrally disposed triangular faces are each capped by an end-on $(\mu_3\text{-}\eta^1\text{-}N_3)$ ligand.

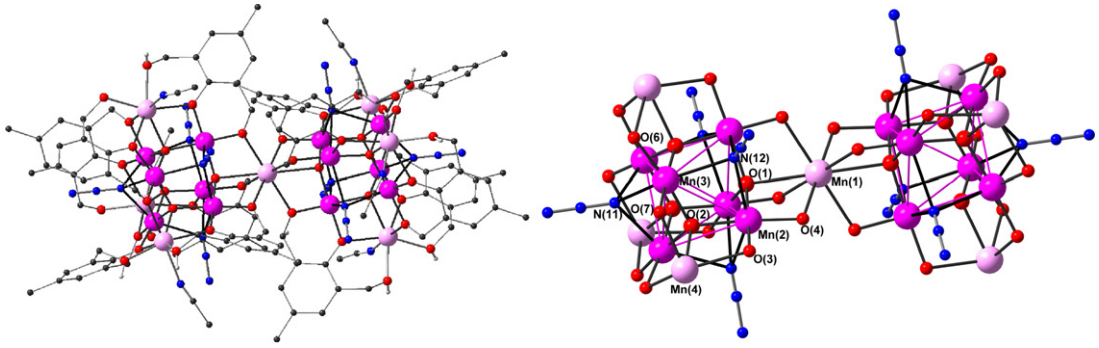

Fig. 8. Molecular structure of the dication $[(HL^{Me})_{12}Mn^{III}{}_{12}Mn^{II}{}_7(\mu_4\text{-}O)_8(\mu_3,\eta^1\text{-}N_3)_8(MeCN)_6]^{2+}$, **$[Mn^{III}_{12}Mn^{II}_7]^{2+}$**, in the crystal (left) and metallic core with partial atom numbering scheme (right). Carbon-bound hydrogen atoms, counter ions, and non-coordinated solvent molecules have been omitted for clarity. Colour code: Mn^{III}, dark pink; Mn^{II}, pale pink; O, red; N, blue.

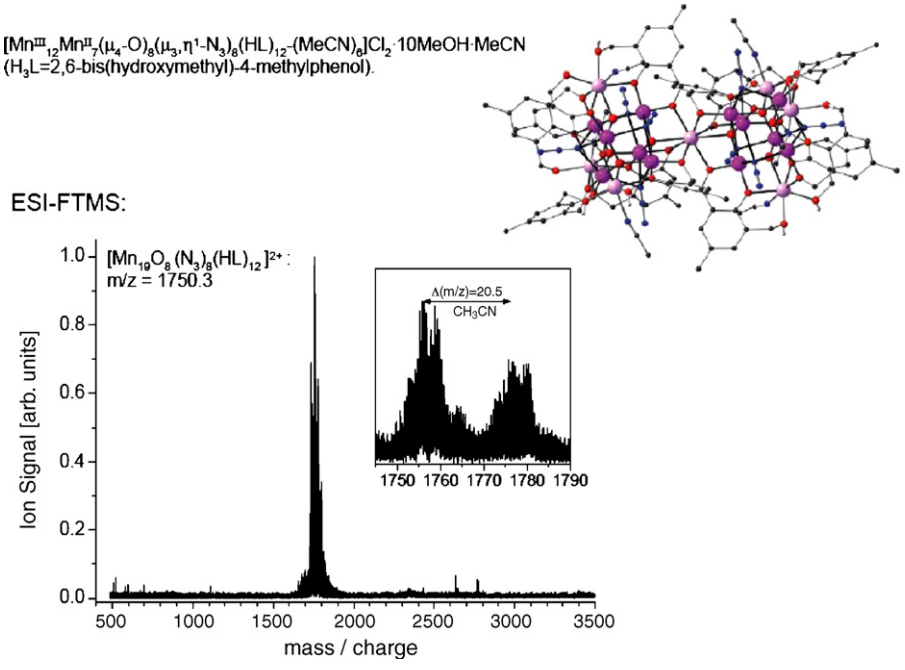

Fig. 9. ESI MS of the **$[Mn_{19}]$**-complex.

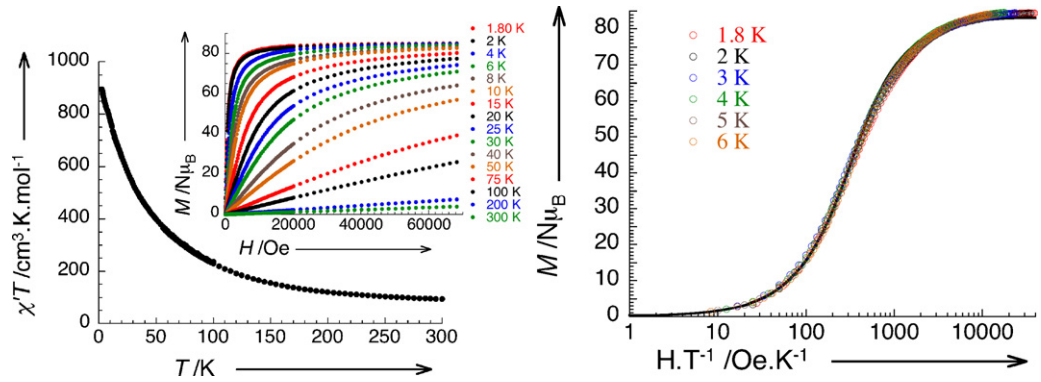

Fig. 10. Temperature dependence of the $\chi'T$ product of $[(HL^{Me})_{12}Mn^{III}{}_{12}Mn^{II}{}_7(\mu_4\text{-}O)_8(\mu_3,\eta^1\text{-}N_3)_8(MeCN)_6]Cl_2$ (where $\chi' = dM/dH$) measured in $H_{dc} = 0$ Oe, $H_{ac} = 3$ Oe and $\nu = 100$ Hz. Inset: field dependence of the magnetization from 1.8 K to 300 K (left); M vs. H/T plot in semi-logarithm plot with data between 1.8 K and 6 K. The solid line is the best fit obtained with an $S = 83/2$ Brillouin function (right).

The remaining four faces are capped by an oxo-ligand, each of which also coordinates to a Mn^{II} center, resulting in a $[Mn^{III}{}_6Mn^{II}{}_4]$ supertetrahedron with a Mn^{II} center at each vertex and a Mn^{III} at the mid-point of each edge. Each Mn^{II}–Mn^{III}–Mn^{II} edge is further supported by a doubly deprotonated $(HL^{Me})^{2-}$ ligand, which forms a phenoxy bridge from the Mn^{III} to one Mn^{II}, and an alkoxy bridge from the Mn^{III} to the other Mn^{II}.

All 12 ligands are in the double-deprotonated form $(HL^{Me})^{2-}$ and coordinate in mode **VIII**, where the protonated BzOH group coordinates to Mn^{II}. The coordination environment of the manganese ions is completed by end-on μ_3-bridging azide ligands. The end-on bridging mode of azide is known to favor ferromagnetic interactions in comparison to the end-to-end bridging mode which favors antiferromagnetic interactions [8].

ESI mass spectrometry investigation established that the core of the **[Mn$_{19}$]**-aggregate is stable in MeOH. As can be seen in the inserted diagram (Fig. 9), essentially a group of peaks are observed around the expected dication at 1750 m/z with a spacing of 20.5 (corresponding to acetonitrile). It is believed that the molecule seem to undergo some "ligand exchange" which is why the mass does not fit perfectly well, but the core of the **[Mn$_{19}$]**-complex does fly without fragmentation.

χT, and thus the effective magnetic moment, μ_{eff}, increases steadily with decreasing temperature indicative of overall ferromagnetic interactions (Fig. 10). Furthermore, magnetization studies confirm that **$[Mn^{III}{}_{12}Mn^{II}{}_7]^{2+}$** possesses an $S_t = 83/2$ spin ground state, indicating that all 83 unpaired electrons in the cluster are aligned parallel. This in turn implies a parallel spin-alignment in the ground state of all 12 Mn^{III} ($S_i = 2$) and seven Mn^{II} ions ($S_i = 5/2$). This $S_t = 83/2$ spin ground state is highest yet realized in a molecule. DFT calculations on the molecule revealed that the Mn(1)–O bond distances are critical to the observed ferromagnetic coupling of Mn(1) to the two $[Mn_9]$ moieties in the $[Mn_{19}]$ aggregate [58]. The unusually large magnetic susceptibility of the compound allows crystals of this molecule to be moved easily at room temperature by using only a simple permanent magnet of 0.35 T.

However, high-frequency EPR study of this molecule showed that D was very small and positive ($D = 0.004\ cm^{-1}$), and concluded

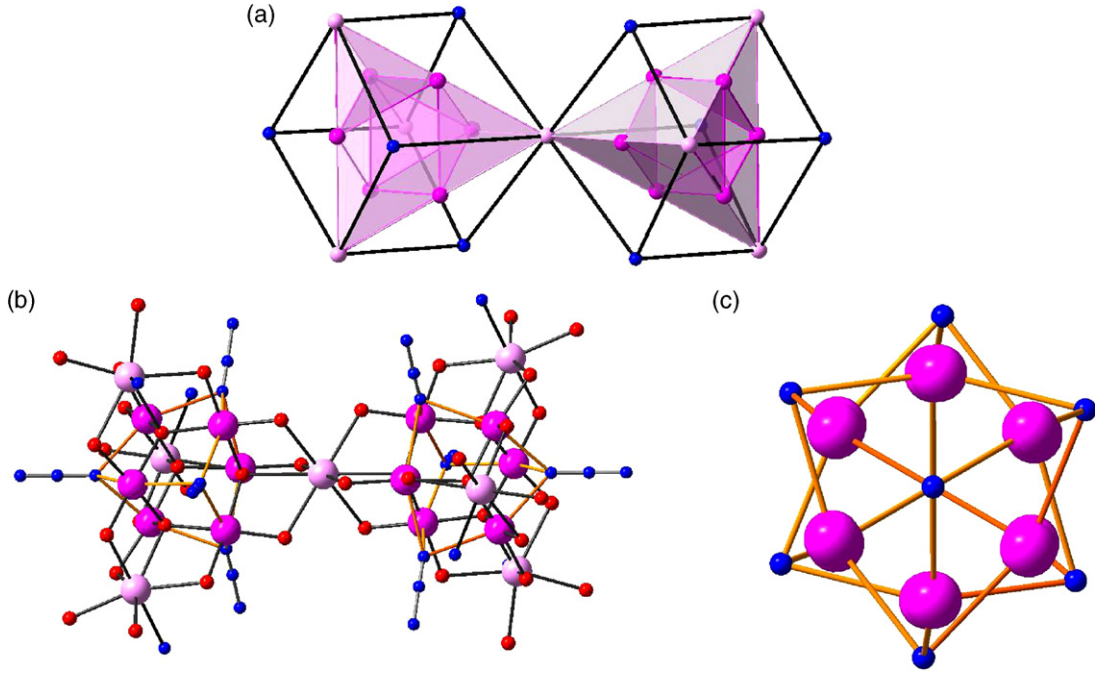

Fig. 11. (a) Polyhedral representation of the core of the aggregate **$[Mn^{III}{}_{12}Mn^{II}{}_7]^{2+}$** emphasising the cubic derived symmetry; (b) highlighted Jahn–Teller axes on the Mn^{III} centers within the core; (c) trigonal arrangement of the Jahn–Teller axes viewed along the crystallographic c axis.

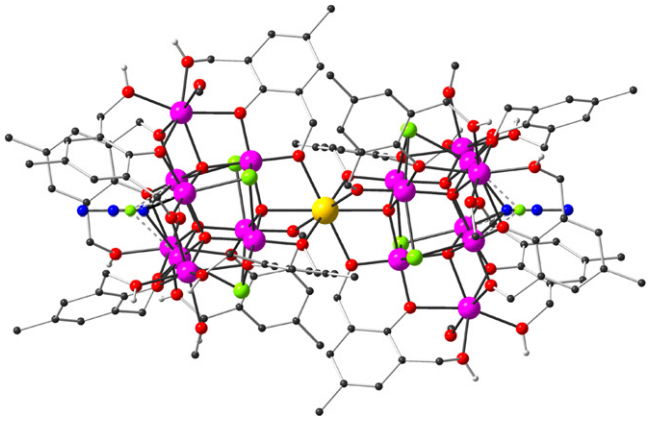

Fig. 12. Molecular structure of **[Mn$_{18}$Dy]** in the crystal. Carbon-bound hydrogen atoms, counter ions and non-coordinated solvent molecules have been omitted for clarity. Bonds to the minor chloride disorder components of the two apical μ_3-ligands are shown dotted. Color code: Mn, pink; Dy, yellow; O, red; N, blue.

that the previously observed magnetic hysteresis loops at very low temperatures probably result from intermolecular dipolar interactions [59].

The molecule presents high symmetry, leading to the almost perfect cancellation of the Jahn–Teller elongated axes on the Mn^{III} centers making up the central octahedron within the supertetrahedron (see Fig. 11) resulting in an overall negligible anistropy for the molecule. This problem is common to manganese(III)-containing clusters which invariably show lower molecular anistropies than would be expected considering a simple tensorial sum of the single ion anisotropies [28].

In order to overcome this lack of molecular anisotropy the rather long Mn–O bond length for the central eight-coordinate Mn^{II} (Mn(1)) suggested a way forward. We reasoned that it might be feasible to replace Mn(1) by lanthanide ions which can provide large spins and/or large magnetic anisotropy, the latter arising from spin–orbit coupling. Hence, we explored the possibility of substituting the central Mn^{II} with lanthanide ions which equally have ionic radius larger than Mn^{II} ions. Addition of a simple lanthanide salt to the reaction mixture that produced the **[Mn$_{19}$]**-aggregate selectively and cleanly replaces the central Mn^{II} to give a **[Mn$_{18}$M]**-aggregate. Exemplarily, the molecular structure of the **[Mn$_{18}$Dy]** analogue is shown in Fig. 12.

The new complex bears a striking structural similarity to the previously reported **[Mn$_{19}$]** [48], as it retains the metallic core topology of the original compound, comprising two vertex-sharing supertetrahedral units. While the two [Mn$_{10}$] supertetrahedra in **[Mn$^{III}_{12}$Mn$^{II}_{7}$]$^{2+}$** share a Mn^{II} vertex, the two tetrahedral units in **[Mn$_{18}$Dy]** now share a Dy^{III} vertex, which again has a distorted octa-coordinate coordination sphere, to give the observed structure in which the complex has $\bar{3}$ crystallographic site symmetry. The Dy^{III} ion introduces uniaxial magnetic anisotropy into the complex as seen from the appearance of out-of-phase ac susceptibility peaks and hysteresis of the magnetization resulting from molecular-based slow magnetic relaxation behaviour [60].

Two closely related tetranuclear manganese complexes of H_3L^{Me} have been reported by Yang et al. [47] The two isostructural, mixed valence complexes $[(HL)_4Mn^{III}_2Mn^{II}_2(MeOH)_4Cl_2]$ and $[(HL)_4Mn^{III}_2Mn^{II}_2(MeOH)_4Br_2]$ contain the doubly deprotonated $(HL^{Me})^{2-}$ ligand, where two ligand molecules coordinate in mode **IV** and the other two ligand molecules coordinate in mode **VIII**. Magnetic measurements establish $S_t = 9/2$ spin ground states with slow relaxation of the magnetization at low temperatures indicating SMM behaviour.

6. Concluding remarks

We have utilized ligands H_3L^R based on 2,6-bis (hydroxymethyl)phenol for the synthesis of titanium, iron, and manganese complexes. The variability in the protonation states and the coordination modes of the ligands allows for the synthesis of complexes with different structures and properties simply by applying small variations in the reaction conditions. In this respect, a dinuclear and a tetranuclear Ti^{IV} complex have been obtained. These two complexes were found to be in a solvent-depending equilibrium. Using iron, a dinuclear, a tetranuclear, and a decanuclear complex have been characterized. All the iron complexes display antiferromagnetic interactions leading to diamagnetic $S_t = 0$ spin ground states. The use of manganese in combination with azide resulted in the formation of a nonadecanuclear mixed valence manganese complex. In this compound the highest possible spin ground state for the system of $S_t = 83/2$ is obtained, which is the record of spin in a molecular compound. Substituting the central Mn^{II} ion in the complex with a Dy^{III} ion introduces uniaxial magnetic anisotropy into the complex and results in slow magnetic relaxation behaviour.

The analysis of the structural properties of the obtained complexes prove the assumption, that ligands based on 2,6-di(hydroxymethyl)phenol are versatile ligands for the construction of high-nuclearity complexes. The rigid backbone does not allow the ligand to act as a tridentate donor to a single metal ion, but rather favors bridging between metal centers. The main protonation state of the ligand is the double-deprotonated form and no compounds have the ligand in the mono-deprotonated form. As a result of a smaller pK_S value the phenol function is always deprotonated and one benzyl alcohol remains protonated. Five different coordination modes of the ligands have been found in these complexes. The deprotonated benzylalcoholate group has a strong tendency to bridge two or more metal ions. Only the use of highly Lewis-acidic metal ions, here Ti^{IV}, results in a terminal coordination mode of a benzylalcoholate ligand. This is due to the strong electron donation necessary to balance the high positive charge of the Ti^{IV} center. This reduces the electron density and therefore the nucleophilicity of the coordinated benzylalcoholate function. However, even with the use of Ti^{IV}, the energies of a terminally coordinated and a bridging benzylalcoholate function are quite similar, which is manifested by the observation of an equilibrium between the **[Ti$^{IV}_2$]$^{-}$** and the **[Ti$^{IV}_4$]$^{2-}$** complexes. The terminal coordination of a benzylalcoholate to Fe^{III}, which is still quite Lewis-acidic, has not yet realized.

In summary, the versatility of the three coordinating groups of the H_3L^R ligands should facilitate the synthesis of many more high-nuclearity clusters, where the exact composition can be varied by changing the pH, the solvent, and by the presence of additional donor ligands. The isolation of the fascinating **[Mn$_{19}$]** and **[Mn$_{18}$Dy]** complexes demonstrates the potential of H_3L^R ligands for the synthesis of complexes with interesting magnetic properties.

Acknowledgements

This work was supported by the Deutsche Forschungsgemeinschaft within the Priority Program 'Moleculuar Magnetism' (SPP1137) and the Fonds der Chemischen Industrie.

References

[1] D. Gatteschi, O. Kahn, J.S. Miller, F. Palacio, Adv. Mater. 3 (1991) 161.
[2] J.S. Miller, A.J. Epstein, Angew. Chem. Int. Ed. Engl. 33 (1994) 385.
[3] E. Coronado, P. Delhaès, D. Gatteschi, J.S. Miller, Molecular Magnetism: From Molecular Assemblies to the Devices, Kluwer Academic Publishers, Dordrecht, 1996.

[4] J.S. Miller, M. Drillon, Magnetism: Molecules to Materials, Wiley-VCH, Weinheim, 2001–2005, vols. I–IV.
[5] J.S. Miller, Inorg. Chem. 39 (2000) 4392.
[6] J.S. Miller, J.C. Calabrese, A.J. Epstein, R.W. Bigelow, J.H. Zhang, W.M. Reiff, J. Chem. Soc., Chem. Commun. (1986) 1026.
[7] J.S. Miller, J.C. Calabrese, H. Rommelmann, S. Chittipeddi, A.J. Epstein, J.H. Zhang, W.M. Reiff, J. Am. Chem. Soc. 109 (1987) 769.
[8] O. Kahn, Molecular Magnetism, VCH Publisher, New York, 1993.
[9] J.M. Manriquez, G.T. Yee, R.S. McLean, A.J. Epstein, J.S. Miller, Science 252 (1991) 1415.
[10] S.M. Holmes, G.S. Girolami, J. Am. Chem. Soc. 121 (1999) 5593.
[11] S. Ferlay, T. Mallah, R. Ouahes, P. Veillet, M. Verdaguer, Nature 378 (1995) 701.
[12] E. Dujardin, S. Ferlay, X. Phan, C. Desplanches, C.C.D. Moulin, P. Sainctavit, F. Baudelet, E. Dartyge, P. Veillet, M. Verdaguer, J. Am. Chem. Soc. 120 (1998) 11347.
[13] T. Lis, Acta Cryst. 36 (1980) 2042.
[14] R. Sessoli, D. Gatteschi, A. Caneschi, M.A. Novak, Nature 365 (1993) 141.
[15] R. Sessoli, H.L. Tsai, A.R. Schake, S.Y. Wang, J.B. Vincent, K. Folting, D. Gatteschi, G. Christou, D.N. Hendrickson, J. Am. Chem. Soc. 115 (1993) 1804.
[16] J.R. Long, in: P. Yang (Ed.), Chemistry of Nanostructured Materials, World Scientific, Hong Kong, 2003, p. 291.
[17] D. Gatteschi, R. Sessoli, J. Villain, Molecular Nanomagnets, Oxford University Press, Oxford, 2006.
[18] D. Gatteschi, R. Sessoli, Angew. Chem. Int. Ed. 42 (2003) 268.
[19] C.J. Milios, A. Vinslava, W. Wernsdorfer, S. Moggach, S. Parsons, S.P. Perlepes, G. Christou, E.K. Brechin, J. Am. Chem. Soc. 129 (2007) 2754.
[20] T. Glaser, M. Heidemeier, T. Weyhermüller, R.-D. Hoffmann, H. Rupp, P. Müller, Angew. Chem. Int. Ed. 45 (2006) 6033.
[21] G. Christou, D. Gatteschi, D.N. Hendrickson, R. Sessoli, MRS Bull. 25 (2000) 66.
[22] J. Tejada, E.M. Chudnovsky, E. del Barca, J.M. Hernandez, T.P. Spiller, Nanotechnology 12 (2001) 181.
[23] J. Tejada, Polyhedron 20 (2001) 1751.
[24] M.N. Leuenberger, D. Loss, Nature 410 (2001) 789.
[25] A. Cornia, A.C. Fabretti, M. Pacchioni, L. Zobbi, D. Bonachi, A. Caneschi, D. Gatteschi, R. Biagi, U. Del Pennino, V. De Renzi, L. Gurevich, H.S.J. Van der Zant, Angew. Chem. Int. Ed. 42 (2003) 1645.
[26] E.D. Dahlberg, Phys. Today 48 (1995) 34.
[27] R.E.P. Winpenny, J. Chem. Soc., Dalton Trans. (2002) 1.
[28] G. Aromi, E.K. Brechin, Struct. Bond. 122 (2006) 1.
[29] S.L. Heath, A.K. Powell, Angew. Chem., Int. Ed. Engl. 31 (1992) 191.
[30] A.K. Powell, S.L. Heath, D. Gatteschi, L. Pardi, R. Sessoli, G. Spina, F. Delgiallo, F. Pieralli, J. Am. Chem. Soc. 117 (1995) 2491.
[31] J.C. Goodwin, R. Sessoli, D. Gatteschi, W. Wernsdorfer, A.K. Powell, S.L. Heath, J. Chem. Soc., Dalton Trans. (2000) 1835.
[32] C.J. Harding, R.K. Henderson, A.K. Powell, Angew. Chem., Int. Ed. Engl. 32 (1993) 570.
[33] A.K. Powell, S.L. Heath, Commun. Inorg. Chem. 15 (1994) 255.
[34] W. Schmitt, C.E. Anson, W. Wernsdorfer, A.K. Powell, Chem. Commun. (2005) 2098.
[35] M. Murusgesu, R. Clérac, W. Wernsdorfer, C.E. Anson, A.K. Powell, Angew. Chem. Int. Ed. 44 (2005) 6678.
[36] A. Mandel, W. Schmitt, T.G. Womack, R. Bhalla, R.K. Henderson, S.L. Heath, A.K. Powell, Coord. Chem. Rev. 192 (1999) 1067.
[37] W. Schmitt, P.A. Jordan, R.K. Henderson, G.R. Moore, C.E. Anson, A.K. Powell, Coord. Chem. Rev. 228 (2002) 115.
[38] R. Robson, Inorg. Nucl. Chem. Lett. 6 (1970) 125.
[39] R. Robson, Austr. J. Chem. 23 (1970) 2217.
[40] D.E. Fenton, H. Okawa, Chem. Ber./Recl. 130 (1997) 433.
[41] E.K. Brechin, J. Yoo, M. Nakano, J.C. Huffman, D.N. Hendrickson, G. Christou, Chem. Commun. (1999) 783.
[42] C. Boskovic, W. Wernsdorfer, K. Folting, J.C. Huffmann, D.N. Hendrickson, G. Christou, Inorg. Chem. 41 (2002) 5107.
[43] A. Rammel, F. Brisach, J. Henry, J. Am. Chem. Soc. 123 (2001) 5612.
[44] T. Glaser, T. Lügger, Inorg. Chim. Acta 337 (2002) 103.
[45] T. Glaser, T. Lügger, R.-D. Hoffmann, Eur. J. Inorg. Chem. (2004) 2356.
[46] T. Glaser, I. Liratzis, T. Lügger, R. Fröhlich, Eur. J. Inorg. Chem. (2004) 2683.
[47] C.I. Yang, G.H. Lee, C.S. Wur, J.G. Lin, H.L. Tsai, Polyhedron 24 (2005) 2215.
[48] A.M. Ako, I.J. Hewitt, V. Mereacre, R. Clérac, W. Wernsdorfer, C.E. Anson, A.K. Powell, Angew. Chem. Int. Ed. 45 (2006) 4926.
[49] K. Hegetschweiler, H. Schmalle, H.M. Streit, W. Schneider, Inorg. Chem. 29 (1990) 3625.
[50] A. Cornia, D. Gatteschi, K. Hegetschweiler, L. HausherrPrimo, V. Gramlich, Inorg. Chem. 35 (1996) 4414.
[51] T. Glaser, T. Beissel, E. Bill, T. Weyhermüller, V. Schünemann, W. Meyer-Klaucke, A.X. Trautwein, K. Wieghardt, J. Am. Chem. Soc. 121 (1999) 2193.
[52] T. Glaser, K. Rose, S.E. Shadle, B. Hedman, K.E. Hodgson, E.I. Solomon, J. Am. Chem. Soc. 123 (2001) 442.
[53] T. Glaser, B. Hedman, K.O. Hodgson, E.I. Solomon, Acc. Chem. Res. 33 (2000) 859.
[54] K. Rose, E.S. Shadle, T. Glaser, S.D. Vries, A. Cherepanow, G.W. Canters, B. Hedman, K.O. Hodgson, E.I. Solomon, J. Am. Chem. Soc. 121 (1999) 2353.
[55] W.H. Armstrong, M.E. Roth, S.J. Lippard, J. Am. Chem. Soc. 109 (1987) 6138.
[56] J.K. McCusker, J.B. Vincent, E.A. Schmitt, M.L. Mino, K. Shin, D.K. Coggin, P.M. Hagen, J.C. Huffman, G. Christou, D.N. Hendrickson, J. Am. Chem. Soc. 113 (1991) 3012.
[57] M.W. Wemple, D.K. Coggin, J.B. Vincent, J.K. McCusker, W.E. Streib, J.C. Huffman, D.N. Hendrickson, G. Christou, J. Chem. Soc., Dalton Trans. (1998) 719.
[58] E. Ruiz, T. Cauchy, J. Cano, R. Costa, J. Tercero, S. Alvarez, J. Am. Chem. Soc. 130 (2008) 7420.
[59] O. Waldmann, A.M. Ako, H.U. Güdel, A.K. Powell, Inorg. Chem. 47 (2008) 3486.
[60] A.M. Ako, V. Mereacre, R. Clérac, W. Wernsdorfer, I.J. Hewitt, C.E. Anson, A.K. Powell, Chem. Commun. (2009), doi:10.1039/b814614d.